대동맥분기에서의 혈액유동:
맥도플러초음파 및 레이저도플러계측기를 사용한 연구

김 영호

Blood Flow in an Aortic Bifurcation Model: Pulsed Doppler Ultrasound and Laser Doppler Anemometry Studies

Young H. Kim
Cardiovascular Flow Dynamics Laboratory, Georgia Institute of Technology

ABSTRACT

In vitro velocity measurements were made using both the pulsed Doppler ultrasound (PDU) machine and laser Doppler anemometer (LDA) system in order to investigate the flow characteristics near the aortic bifurcation. Velocities measured from the PDU machine was in good agreement with those from the LDA. The flow in the daughter branches was three-dimensional with a secondary flow. The oscillating wall shear stress with this secondary fluid motion is well correlated with the localization of the atherosclerosis.

INTRODUCTION

Atherosclerosis is a degenerative disease of the arteries characterized by the proliferation of connective tissue and accumulation of lipids in the intima of arterial wall immediately under the endothelial layer that lines the lumen. Atherosclerotic plaques tend to appear preferentially in certain areas of the arterial tree.

The abnormal wall shear stress is believed by many investigators to be the principal fluid mechanical mediator of atherosclerosis. Fry [1] postulated with his experimental results in dog that increased wall shear stress could damage endothelial layer to develop atheroma. On the other hand, Caro [2] suggested based on the intraluminal mass transfer process that atherosclerosis could develop in regions of low shear stress. Whether the abnormal flow pattern results directly from high or low shear stress on the arterial wall is still unknown. In order to elucidate the exact role of the wall shear stress in the development of the atherosclerotic plaques in arterial walls, a precise knowledge of hemodynamics in arteries is required.

In order to develop a better understanding of the characteristics of the flow near the bifurcation, several investigators have performed theoretical and experimental studies. Experimental works involved flow visualizations [3-8], velocity measurements [9-12], and wall shear stress measurements [13,14]. The LDA method has been used as a gold standard method to measure the in vitro velocity with an accuracy. Recently, PDU machines are available in measuring the flow rates and velocities along the vessel both in vivo and in vitro. The aims of the present study is to understand the flow dynamic fields in the aortic bifurcation and to compare the PDU results with the LDA results.

METHODS

The experimental model was fabricated from the cast of human aortic bifurcation of methyl methacrylate. It was enlarged about 1.5 times compared to the natural size. Figure 1 shows the sketched Plexiglas model of the aortic bifurcation with a bifurcation angle of 53°.

Pulsed Doppler Ultrasound Studies

Pulsed Doppler ultrasound velocity profile measurements were made with 10 MHz needle probes interfaced with the VingMed SD-100 ultrasound Doppler system. At each site, the sample volume (1 mm^3 in size) of the intraluminal probe (about 2 mm in diameter) was located in the place of interest and the ultrasound crystal oriented such a way that the ultrasound beam is parallel to the main direction of the flow. The Doppler spectral data was obtained using a fast Fourier transform algorithm on the SD-100 system.

Laser Doppler Anemometer Studies

A 55X modular three-beam DISA (Dantec) LDA system was used for the present study. A schematic diagram of the LDA system is briefly shown in Figure 2. The He-Ne laser beam enters the LDA optical system, which comprises of a mounting bench, two beam splitter sections, a Bragg cell, a beam displacer, a beam translator, a front lens and two photomultiplier tubes. Three beams that emerges from the lens are focused onto the sample volume so as to intersect each other. The digital output from the counter was interfaced with PDP 11/03 minicomputer via buffer interface. The traverse mechanism permitted the movement of measuring volume along any mutually orthogonal axes. The distance traveled in each direction to a fixed origin in an accuracy of 0.04 mm. The fast Fourier transform (FFT) was used to analyze the velocity data.

For steady flow measurements, mean Reynolds number of 950 was used in both studies. The mean Reynolds number of the pulsatile flow was approximately 400 and corresponding mean velocity was about 23 cm/sec with an oscillating velocity amplitude of 34 cm/sec. Womersley number of 13.6 was employed for the pulsatile flow. Both measurements were taken at the acceleration phase in the systole, peak systole, and deceleration phase in the systole, which is shown as the flow waveform in Figure 3.

RESULTS AND DISCUSSION

Steady Flow

Figure 4 shows the nondimensionalized axial velocity profiles in the steady flow. Velocity profiles in the mother branch proximal to the bifurcation is relatively blunt . In the daughter branch, due to the sudden change in the flow direction, the fluid was subject to a centrifugal force and pushed towards the inner wall. This skewness of the velocity profile in the daughter branches disappeared at the downstream location of the daughter branches. It is noted that the velocity profile had a double peak just distal to the bifurcation, which was previously reported by Schroter and Sudlow [14]. This is due to the secondary flow in the daughter branches. The outward motion of the flow in the daughter branch pushed the maximum velocity towards the outer wall. This also results in the secondary fluid motion like horseshoe vortex in the daughter branches. Therefore, the high shear region located at the inner wall and low shear region placed distally at the same axial location at the outer wall. This secondary motion of the fluid depends upon the Reynolds number and the geometric factors such as the bifurcation angle and the size of the daughter vessel.

Pulsatile Flow

Figure 5 shows the axial velocity profiles at various locations during the systolic acceleration phase using PDU and LDA techniques. Velocity profiles in the mother branch were relatively blunt and had a M shape which appeared to be more significant as the fluid approached proximal to the vertex in the mother branch. Velocity profiles in the daughter branch are also skewed toward the inner wall due to the centrifugal force, but they were quickly dampened out due to the pulsatile nature of the flow compared to the steady flow. On the other hand, due to the damping of the branching effect, pressure drop and the energy loss are probably less important for the pulsatile flow. During peak systole, as shown in Figure 6, axial velocity profiles reached the maximum values and the skewness toward the inner wall in the daughter branches was more pronounced. Figure 7 represents the velocity profiles during the deceleration phase of the systole. M-shaped velocity profile close to the vertex in the mother branch became more significant at this stage. A flow separation was observed along the outer wall of the daughter branches.

A small inward displacement of the maximum velocity along the daughter branches is probably the most distinguished effect, compared to the steady flow. This effect is particularly important because high shear stresses and corresponding thrombosis can be localized along the inner wall of the vessel. The results using PDU and LDA techniques were in good agreement each other during the cardiac cycle. Flow in the daughter branches is essentially three-dimensional with a secondary flow. During the systole, high wall shear stress was localized along the inner wall in the daughter branches, and on the other hand, low shear was placed distal to the vertex along the outer wall. This oscillating wall shear stress with a secondary flow motion is important in determining the development of thrombosis and atherosclerotic plaques.

CONCLUSIONS

The flow dynamics near the model aortic bifurcation was studied using PDU and LDA methods. Axial velocity profiles from both measurements are quite in good agreement except very near the wall. The results demonstrated the flow separation and formation of paired secondary flow which might effect local mass transfer and interactions of blood cells with the vessel wall leading to the localization of thrombosis and atherosclerosis in this region.

REFERENCES

1. Fry DL (1968): Acute vascular endothelial changes associated with increased blood velocity gradients. Circ. Res. 22:165-197.

2. Caro CG, Fitz-Gerald JM, Schroter RC (1971): Atheroma and arterial wall shear: Observation, correlation and proposal of a shear dependent mass transfer mechanism for atherogenesis. Proc. Royal Soc. Lond. B117:109-159.

3. Roach MR (1977): The effects of bifurcation and stenoses in arterial disease. Cardiovascular dynamics (Hwang NHC and Normann NA eds), University Park Press, Baltimore.

4. Fukushima T, Homma T, Azuma T, and Harakawa K (1987): Characteristics of secondary flow in steady and pulsatile flow through a symmetrical bifurcation. Biorheology 24:3-12.

5. Walburn FJ, Sabbah HN and Stein PD (1981): Flow visualization in a mold of the human abdominal aorta. ASME J. Biomechanical Eng. 103:168-170.

6. Bharadvaj BK, Mabon RF and Giddens DP (1982): Steady flow in a model of the human carotid bifurcation Part 1. Flow visualization. J. Biomech. 15:349-362.

7. Karino T and Goldsmith HL (1985): Particle flow behavior in models of branching vessels II. Effects of branching angle and diameter ratio on flow patterns. Biorheology 22:87-104.

8. Back MR, Cho YI, Crawford DW and Back LH (1987): Fluid particle motion and Lagrangian velocities for pulsatile flow through a femoral artery branch model. ASME J. Biomechanical Eng. 109:94-101.

9. Rieu R, Friggi A and Pelissier R (1985): Velocity distribution along an elastic model of arterial tree. J. Biomech. 18:703-713.

10. Ku DN, Giddens DP (1987) Laser Doppler anemometer measurements of pulsatile flow in a model carotid bifurcation. J. Biomech. 20:407-421.

11. Sung HW, Philpot EF, Nanda NC and Yoganathan AP (1990) Axial flow velocity patterns in a pulmonary artery model with varying degrees of valvular pulmonic stenosis: Pulsatile in vitro studies. J. Biomech. 23:562-578.

12. Rindt CCM, Von Steenhoven AA and Renemann RS (1988): An experimental analysis of the flow field in a three-dimensional model of the human carotid artery bifurcation. J. Biomech. 21:985-991.

13. Ku DN, Giddens DP, Zarins CK and Glagov S (1985): Pulsatile flow and atherosclerosis in the human carotid bifurcation: Positive correlation between plaque location and low and oscillating shear stress. Arteriosclerosis 5:293-302.

14. Schroter RC and Sudlow MF (1969): Flow patterns in models of the human bronchial airways. Respir. Physiol. 7:341-355.

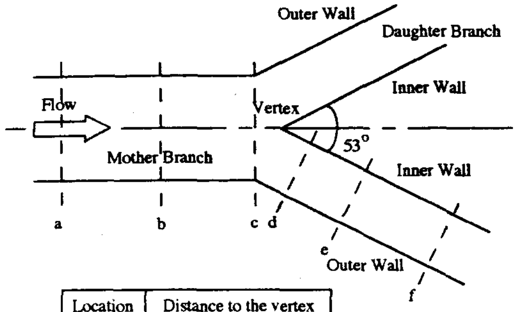

Location	Distance to the vertex
a	0.4 D proximal
b	1.6 D proximal
c	3.6 D proximal
d	0.25 D distal
e	0.8 D distal
f	1.5 D distal

Figure 1. Plexiglass model the aortic bifurcation.

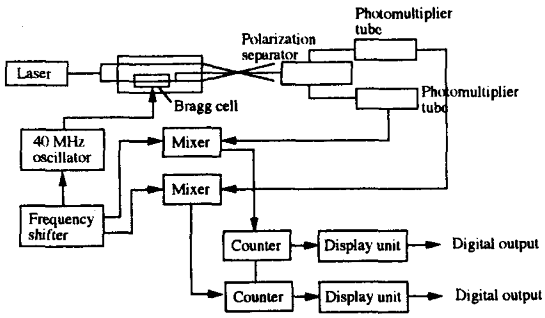

Figure 2. Schematic of three-beam LDA system.

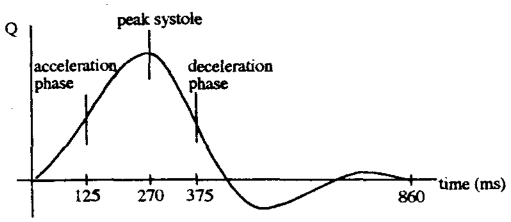

Figure 3. Flow waveform and the time information for data collection.

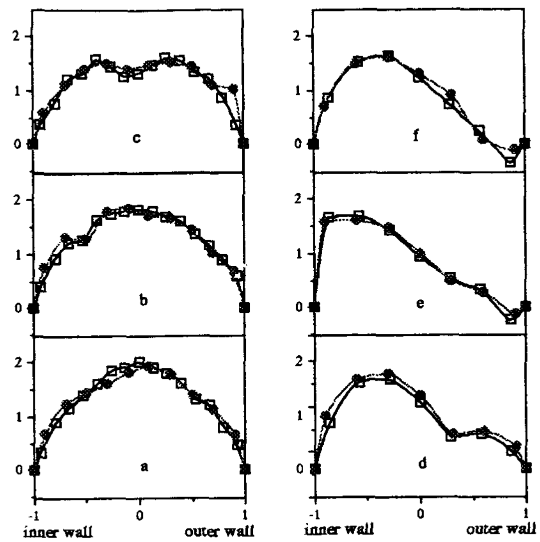

Figure 4. Nondimeionalized axial velocity profiles in steady flow.
a - f correspond to the location where the measurement was made. (Refer to Figure 1.)

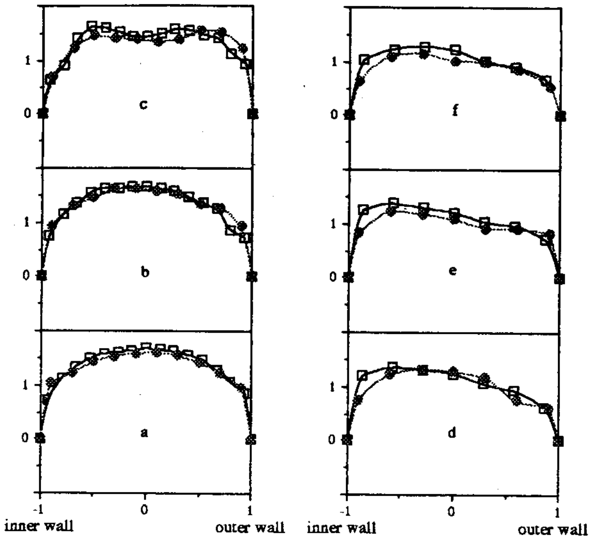

Figure 5. Nondimensionalized axial velicity profiles at various locations during the acecleration phase. a - f correspond to the location where the measurement was made. (Refer to Figure 1.)

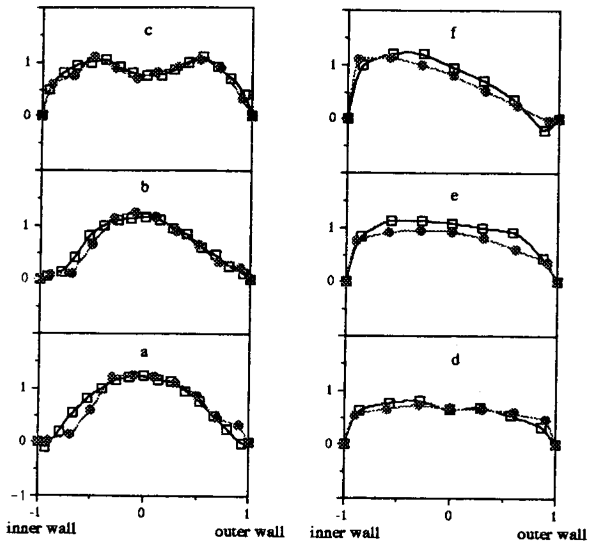

Figure 7. Nondimensionalized axial velicity profiles at various locations during the deceleration phase. a - f correspond to the location where the measurement was made. (Refer to Figure 1.)

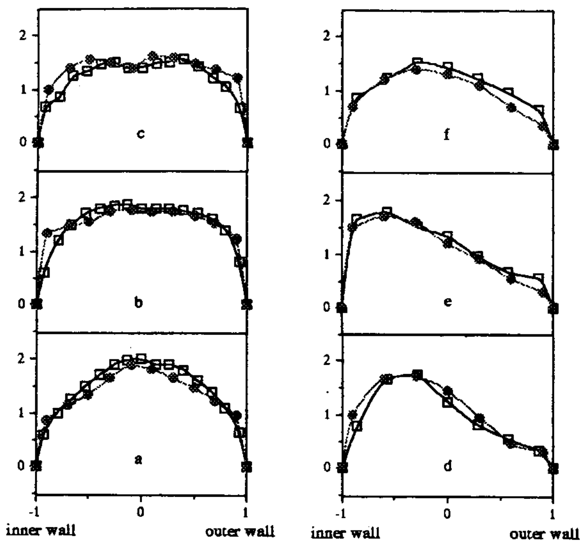

Figure 6. Nondimensionalized axial velicity profiles at various locations during the peak systole. a - f correspond to the location where the measurement was made. (Refer to Figure 1.)